Analysis of a Nailed Soil Slope Using Limit Equilibrium and Finite Element Methods – A Review

Nur Irfah Mohd Pauzi[1*], *Mohd Shahril* Mat Radhi[2], and *Thang* Kel Win[3]

[1, 3]Institute of Energy Infrastructure (IEI), Civil Engineering Dept., College of Engineering, 43009, Universiti Tenaga Nasional (UNITEN), Malaysia
[2]George Kent (Malaysia) Berhad, George Kent Technology Centre, 1115 Jalan Puchong, Taman Meranti Jaya, 47120 Puchong, Selangor, Malaysia

Abstract Reviewing the two most used techniques for slope stability analysis is the goal of this research. The analysis derived from PLAXIS 2D (finite element based) and SLOPE/W (limit equilibrium based). Two 45-degree and 60-degree slope angles that are strengthened with nails at three different inclinations—0, 15, and 30—are used for the analysis. All nail inclinations and slope angles are measured from the horizontal. A comparative analysis of stability metrics, including critical slip surfaces, nail forces, and factor of safety, has been conducted. It is discovered that the limit equilibrium approach produces greater values of the factor of safety when compared to the finite element method. There are notable differences between the failure surfaces obtained from the two methods.Large nail forces are seen using the LEM approach for 45 slopes with all nail inclinations, however the FEM method indicates an increase in the nail forces for 60 slope angles. In conclusions, both FEM and LEM methods have advantages and disadvantages. These two methods give the precise results if both methods are combined. The analysis using the LEM to compute the factor of safety are further enhanced with the Finite Element using PLAXIS 3D to compute the stress strain displacement of the soil with added soil nailing or structure member such as retaining wall.

1 Introduction

Soil nailing has emerged as an effective ground improvement technique especially in cases of slope instability. The unstable slopes can now be improved and made stable using soil nailing technique. It is necessary to examine the stability and methods of reinforcement of these reinforced slopes. Many scholars [1-4] have used the standard limit equilibrium approach to analyze the stability of reinforced slopes. These limit equilibrium techniques, also referred to as the "method of slices," are predicated on the idea of calculating the factor of safety by slicing the failure mass into slices and making certain assumptions about the interslice force distribution. The pre-selected slip surface of an assumed geometry, such as a

* Corresponding author: irfah@uniten.edu.my

wedge, circular, or log-spiral, and the inclination or position of the interslice forces are typically the focus of the assumptions [5].

Researchers have also used limit analysis, which consists of an upper bound approach and a lower bound approach, in addition to the limit equilibrium method (LEM). The analysis of the lower bound technique [6, 7] includes static acceptable stress fields, which are typically assumed and have no meaningful relationship to the actual stress fields. Therefore, finding the lower bound solutions to a real-world slope problem is difficult. Because the kinematically admissible velocity fields in the upper bound approach are created by a stiff element, the limit analysis of slope stability is appropriate for complex situations such slopes with intricate geometries, profiles, groundwater conditions, and loadings. [8–10]. However, to find the best upper bound solution for structures and geotechnical issues, other methods have also been employed, such as special sequential quadratic programming, linear finite elements, non-linear programming, and stiff finite elements. [11].

In order to forecast the real site conditions, the finite element technique (FEM) [12] is also utilized to analyze the failure zone, soil non-linearity, and the staged building effect [13]. The application of the finite element method to numerical modeling of reinforced slopes has shown to be highly beneficial in the following areas: stress analysis [14], nail pullout resistance [15, 16], nail forces along nail length, nail force variations with cohesion, angle of friction, and lateral movement of the slope [17–20]. The strength reduction approach can also be used to calculate the factor of safety using finite elements. [21–23].

By reducing the strength parameters (phi and c) by the safety factor, the strength reduction method (SRM) analysis applies body forces resulting from soil weight and other external loads until the system is unable to maintain a stable condition [24]. Numerous well-known commercial geotechnical finite element or finite difference programs, including PLAXIS 2D, SNAIL, ANSYS, and FLAC 2D, also use this technique [25]. The pseudo-static stability issues in a frictional-cohesive material have also been resolved through the application of the strength reduction technique. [26]. Gurocak et al. [27] used a two-dimensional (2D) finite element program to apply the strength reduction method to rock slope stability analysis. The impact of soil–nail interaction is not sufficiently taken into account, despite the fact that 2D analysis offers insightful information about the behaviour of nailed slopes.

Additional techniques, such as artificial neural networks (ANN), have been developed recently to investigate the deformation of soil-nailed walls [28]. Nowadays, stresses are measured utilizing Fiber Bragg grating (FBG) sensing technology to carry out the factor of safety computation [29]. Esmaili [30] measured the displacement of soil nail walls using close-range photogrammetry. Reliability analysis based on the Monte Carlo simulation technique is also used to evaluate the sliding stability and global stability of soil nail walls versus ultimate limit states [31]. Statistical techniques, the different element analysis method (DEM) and the adaptive neuro fuzzy inference system (ANFIS) are also used in the analysis of reinforced slope stability[32].

2 Methodology of the Research

This work uses the software packages SLOPE/W and PLAXIS 2D v8.1 to analyze the response of soil-nailed slopes, with the goal of highlighting potential discrepancies between the two most used slope stability approaches (LEM and FEM). The experimental study on nailed soil slope at varied slope angles of 45 o and 60 o, utilizing nail inclinations of 0 o, 15 o, and 30 o with the horizontal, conducted by Rawat and Gupta [15] has been numerically

modeled. The experimental findings from Rawat and Gupta [15] are analyzed and used to validate the comparison of the factor of safety, failure slip surfaces, and nail forces from LEM and FEM.

2.1 Reinforced Slope Stability Analysis Using Limit Equilibrium Method

The interaction between the soil and the structure largely determines how reinforced systems respond. the relationship between the structural elements (nails), which aid in the load transmission mechanism, and the soil, which supplies both mobilizing and resistive stresses. By guaranteeing the system's static equilibrium, the general limit equilibrium technique offers a global factor of safety for the final limit state [5]. Two types of factors of safety and interslice shear-normal forces are used in the factor of safety calculation derived by the general limit equilibrium (GLE) or merely limit equilibrium (LE) technique.

(a) Factor of safety with respect to moment equilibrium (Fm)

$$F_m = \frac{\sum(c'\beta R + (N - u\beta)R\tan\phi')}{\sum Wx - \sum Nf \pm \sum Dd} \qquad (1)$$

(b) Factor of safety with respect to force equilibrium (Ff)

$$F_f = \frac{\sum(c'\beta\cos\alpha + (N - u\beta)\tan\phi'\cos\alpha)}{\sum N\sin\alpha - \sum D\cos\omega} \qquad (2)$$

The normal force at the base of each slice (N) is the major variable in both equations of factor of safety. The value of this normal force is dependent on the shear forces (XL and XR) acting on the slices of the slopes. The base normal force is obtained by the relation:

$$N = \frac{W + (X_R - X_L) - \left(\frac{c'\beta\sin\alpha + u\beta\sin\alpha\tan\emptyset'}{F}\right)}{\cos\alpha + \frac{\sin\alpha\tan\emptyset'}{F}} \qquad (3)$$

The calculations of both Factor of Safety for moment equilibrium and force equilibrium using the equations are Limit Equilibrium Method (LEM) method. This LEM method is further analysed to add the soil nailing using the Finite Element Method (FEM).

2.2 Reinforced slope stability analysis using finite element method

The slip surface for 45 degrees slopes is analysed with 3 different degree of inclination which is 00, 150 and 300 of soil nailing. The analysis of the slopes are shown in Figure 1. The finite element (FE) method has gained widespread acceptance for the analysis of slope stability due to its advantage of not requiring assumptions regarding the location of the failure surface and interslice forces [12]. Analysis is now nonlinear and iterative due to the growing utilization of complicated geometries and material data. In these situations, the inputs—geometry and soil—are functions of the solutions themselves. Utilizing the existing FE packages is advised because this process necessitates a significant quantity of computation time and data. The PLAXIS 2D v8.1 FE software package is one such program that was

utilized in the current investigation. Using FE analysis, this software separates the continuum into discrete parts, which are then further subdivided into nodes.

The degree of freedom for each node in the issue with a specified set of boundary conditions corresponds to the unknowns [13]. The degree of freedom of the nodes is connected to displacement components in the current work. Three nodes are separated into each line element, and each node is given a displacement value. In contrast, if the line element has five nodes, it creates a 15-noded triangle. These three nodes add to the six node triangles. When it comes to nails, anchors, or geogrids, it has been discovered that the 15-noded triangles produce more accurate results than the six-noded triangles. [13].

The tiny incremental stress and strain relationship also governs the material in the FE analysis. The constitutive model of Mohr-Coulomb is used in the FEM package. This procedure mimics the formation of irreversible strains in a perfectly pliable material environment. Plastic point occurrence in the continuum is checked by generating a series of yield functions that make up a yield surface. These yield functions are self-existent. based on the current levels of strain and stress. Additionally, the FEM procedure makes it possible to model the material's elastic, totally plastic behavior. To link the stress to the strains, apply Hooke's law. During calculations, these strains and the strain rates are broken down into their elastic and plastic fractions. According to Griffith and Smith [33], the Mohr–Coulomb model is made up of six yield functions that are made up of the soil's plastic characteristics, such as "c" and "phi."

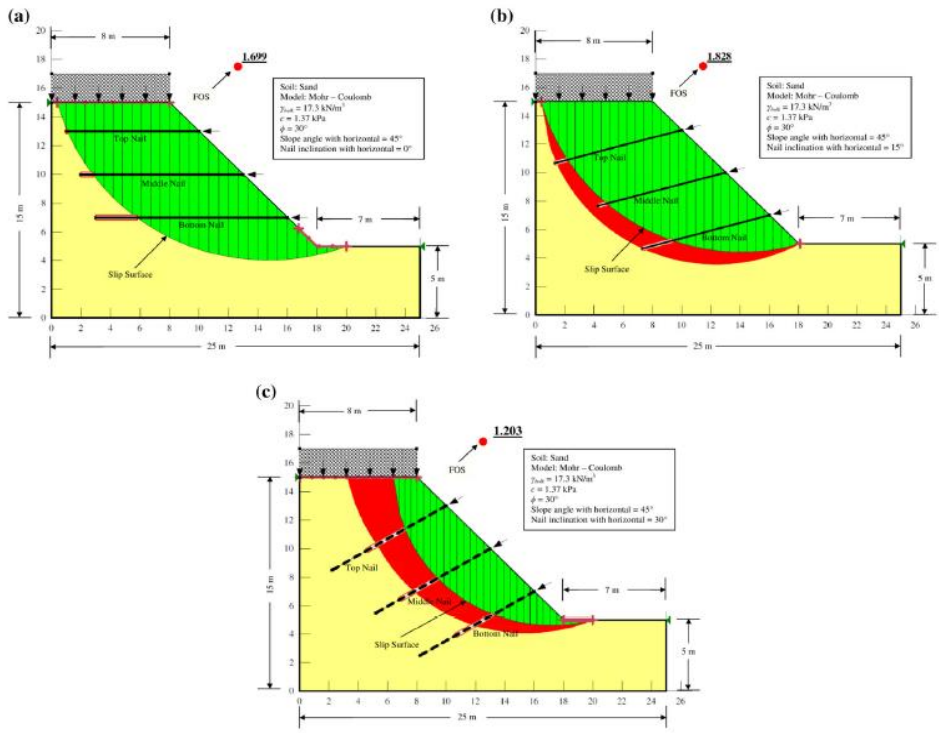

Fig. 1. a Slip Surface for 45° slope for 0 ° nail inclination. **b** Slip Surface for 45 ° slope for 15 ° nail inclination. **c** Slip Surface for 45 ° slope for 30 ° nail inclination. Rawat S and Gupta AK, (2016)

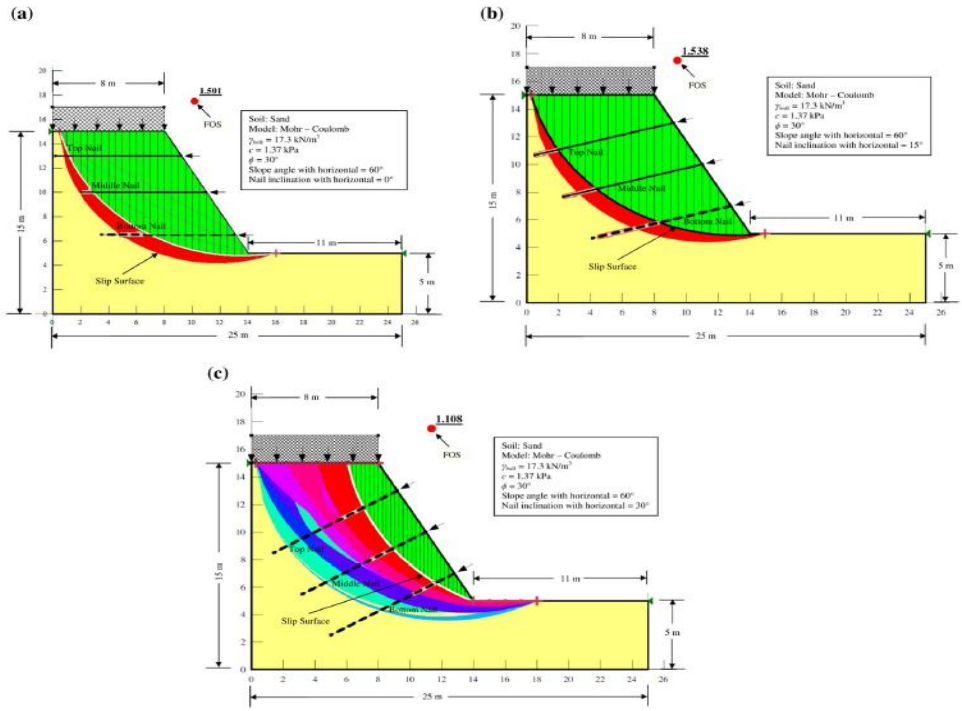

Fig. 2 a Slip Surface for 60º slope for 0 º nail inclination. **b** Slip Surface for 60 º slope for 15 º nail inclination. **c** Slip Surface for60 º slope for 30 º nail inclination. Rawat S and Gupta AK, (2016)

The FE analysis creates a material stiffness matrix using these ideas for material transition in order to determine the stiffness of each component and eventually the total volume of soil. It has also been noted from the literature review that in order to determine the factor of safety for slopes, researchers [34, 35] used the FE strength reduction approach. The convergence criterion is the most important consideration when evaluating the factor of safety in strength reduction analysis. The strength reduction method, sometimes referred to as the /–c reduction method, involves a series of load advancement steps. Through the use of an incremental multiplier Msf, the strength parameters are reduced. The following formula is used to determine the safety factor:

$$SF = \frac{Available\ strength}{strength\ at\ failure} = value\ of\ \sum M_{sf}\ at\ failure. \tag{4}$$

The type of constitutive soil model chosen, the element's type and size, the discretized mesh, the displacement curve's node location, and the tolerance permitted for non-linear analysis all affect how accurate the factor safety is. The model is said to have reached the final state, depending on which FE routine was chosen, if either the maximum number of iterations is reached, the model has experienced a continuous failure mechanism, or the displacement at selected points in the continuum is suddenly changed. FEM packages additionally include the use of arc-length control in the iteration procedure to accurately model the failure. Occasionally, when doing a non-linear analysis, some points suddenly fail toobserved which lead to the generation of an ‘‘apparent’’ negative stiffness matrix beyond the ultimate limit

condition. The arc-length control technique has solved the snap through issue in FEM. The commercial finite element program PLAXIS now includes the arc-length control technique to provide dependable collapse loads for load-controlled calculations. Hence, the study uses PLAXIS 2D, a dependable and effective method for determining the factor of safety of slopes, which is based on the finite element method and combined with an elastic completely plastic (Mohr–Coulomb) stress–strain relation.

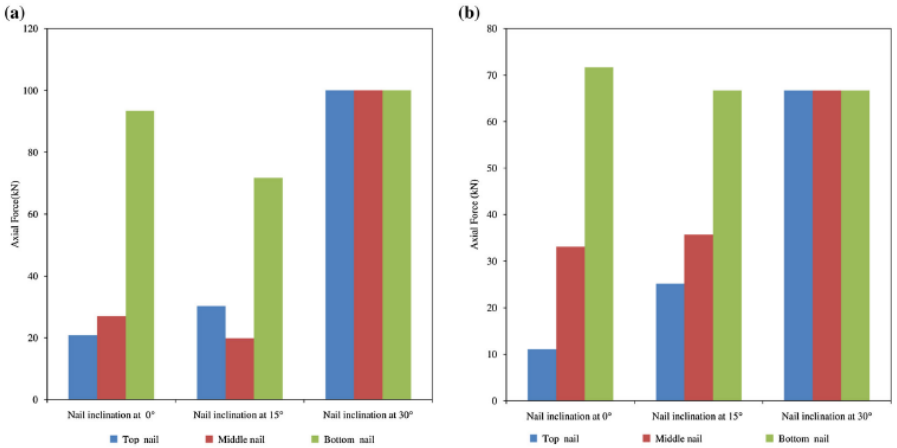

Fig. 3 a Axial force distribution in top, middle and bottom nails with different nail inclinations for 45 º slope. **b** Axial force distribution in top, middle and bottom nails with different nail inclinations for 60 º slope. Rawat S and Gupta AK, (2016)

Table 1 Summary of the nail length mobilized (Rawat S, Gupta AK ,2016)

Slope angles with horizontal (°)	Nail inclinations with horizontal (°)	% age nail length used		
		Top nail	Middle nail	Bottom nail
45	0	99.73	98.80	93.60
	15	91.20	90.80	87.33
	30	45.07	48.67	42.80
60	0	98.27	94.80	89.73
	15	87.47	85.20	77.33
	30	30.80	27.47	24.67

2.3 Numerical modelling and analysis using PLAXIS 2D

The FE method PLAXIS 2D v8.1 has been used to numerically simulate reinforced slopes. Using a 15-noded triangulation process, PLAXIS 2D takes into account the soil slope in plain strain. The model's dimensions align with the ones used in LE analysis. The real boundary conditions of the model test carried out by Rawat and Gupta (2016) are simulated using the standard fixities. Using the usual fixities, the back of the slope is constrained solely in the x-direction, while the model's base is restricted in the x–y direction. To simulate the model in FEM, a Mohr–Coulomb model with well-graded sand soil is employed. The phreatic line is placed at the base of the model to represent the drained soil condition. Table 4 provides a summary of the parameters used in the slope and nail modeling. Plate elements, geogrids, node to node anchors, and fixed end anchors are available as reinforcement systems with the

PLAXIS package. But for slope reinforcement, nails can be substituted by an elastic equivalent plate element. According to the literature review [FHWA, 2012; Shiu and Chang, 2006; Fan and Luo, 2008], the simulation of nails is significantly influenced by the bending and axial stiffness. For an accurate simulation of the soil nails, equivalent flexural rigidity and equivalent axial stiffness must be computed if the nails are modeled using a plate element with a circular cross section. Babu et al. [16] provide the following formula to get the equivalent modulus of elasticity for the simulated nails:

$$E_{eq} = E_n \frac{A_{nail}}{A} + E_g \frac{A_{grout}}{A} \tag{5}$$

Similarly Equivalent axial stiffness is given by

$$EA = \frac{E_n}{S_h} \frac{\Pi}{4} d_n^2 \tag{6}$$

The equivalent bending stiffness is calculated by the relation:

$$EI = \frac{E_n}{S_h} \frac{\Pi}{64} d_n^4 \tag{7}$$

The equivalent plate diameter of the nail is calculated by the PLAXIS software using the formulation:

$$d_{eq} = \sqrt{12\left(\frac{EI}{EA}\right)} \tag{8}$$

In this work, the nail input values used for the analysis are determined using the Eqs. (4), (5), (6), and (7), as indicated in Table 2. The adoption of an interface with a virtual thickness factor (d) of 0.1 ensures appropriate soil–nail interaction. During the mesh generation process, this virtual thickness factor is multiplied by the element thickness. The material data set assigned to the model is also assigned to the interface. In the absence of experimental data, an interface strength reduction factor (Rinter) with a value of 2/3 is utilized to simulate pullout resistance in soil nails. It connects the soil's strength to the interface's strength as

$$\frac{\tan \phi_{interface}}{\tan \phi_{soil}} = R_{inter} \text{ and } \frac{c_{interface}}{c_{soil}} = R_{inter} \tag{9}$$

Following the modeling of the soil-nail interactions, a 2D mesh is produced once the initial stresses are calculated using the Ko technique and Janbu's relation, Ko = ¼ ð1 sin/\. To get precise findings, a finer 2D mesh is created at the soil–nail contacts. The current research does not take pre-overburden pressure or over-consolidation into account. The /–c reduction approach is used to analyze the simulated model (SRM). When slope failure is reached, this calculating approach produces an incremental multiplier PMsf value as results converge. For the reinforced slope failure, this incremental multiplier number is regarded as FOS. Fig. 6 displays the entire slope of reinforced soil that has been simulated.

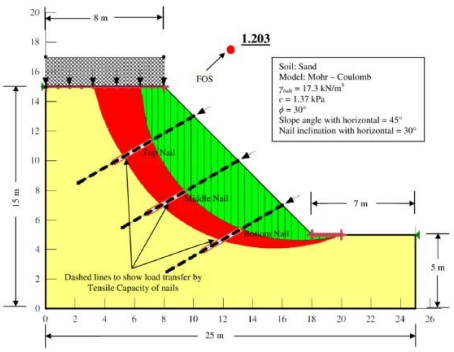

Fig. 4 Slope stability by tensile capacity of nails in 45° slope with 30° nail inclination inclination

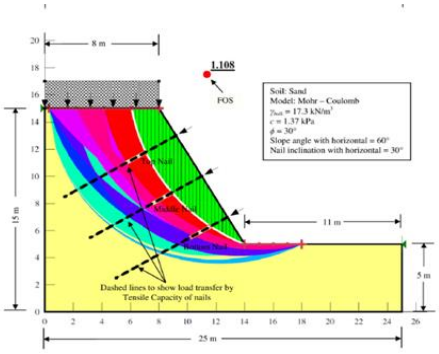

Fig. 5 Slope stability by tensile capacity 60° slope with 30° nail

Table 2 Material properties used in numerical modelling (Rawat S, Gupta AK ,2016)

Properties		Stiffness		Alternate stiffness		Strength	
Simulated model	Plain strain	E_{ref}	50,000 kN/m^2	G_{ref}	115,400 kN/m^2	c_{ref}	1.37 kN/m^2
Elements	15-node	υ	0.3	E_{oed}	403,800 kN/m^2	ϕ	30°
Model type	Mohr–Coulomb					ψ	0°
Material type	Drained						
γ_{unsat}	13.6 kN/m^3						
γ_{sat}	19.68 kN/m^3						
K_o	0.5						

3 Results from PLAXIS 2D Finite Element Method

3.1 Factor of Safety from PLAXIS 2D

According to PLAXIS 2D, a 45-degree slope reinforced with a 15-degree nail inclination produces a maximum factor of safety of 1.43. The factor of safety is determined to be 1.36 and 1.15 for each of the remaining inclinations of 0 and 30 degrees, respectively. Figure 7 illustrates how the factor of safety increases with slope displacement under surcharge for a 15 o nail inclination, reaching a total displacement of 0.462 m of slope. Additionally, Figures 7 and 8 show that the minimum factor of safety for a 30 o nail inclination in a 45 o and 60 o slope is 1.08 and 1.15, respectively. Additionally, Figure 7 indicates that, in comparison to nail inclinations providing the largest FOS, nail inclinations with the least factor of safety fail at a comparatively lower displacement. For a 45-degree slope, an intermediate factor of safety value of 1.36 is associated with a nail inclination of 0 degrees, and for a 60-degree slope, 1.17. It's also crucial to note that, for a 60-degree slope, the factor of safety climbs quickly for tiny displacements of 0.1 m and then stays constant until the slope displacement increases to the point of failureAt a 15 o nail inclination, the greatest factor of safety for 60 o is 1.37. Like a 45-degree slope, 0 and 30 degrees have significantly lower safety factor ratings. It is discovered that a nail inclination of 30 degrees has the lowest safety factor for a 60-degree slope, which coincides with a 45-degree slope angle.

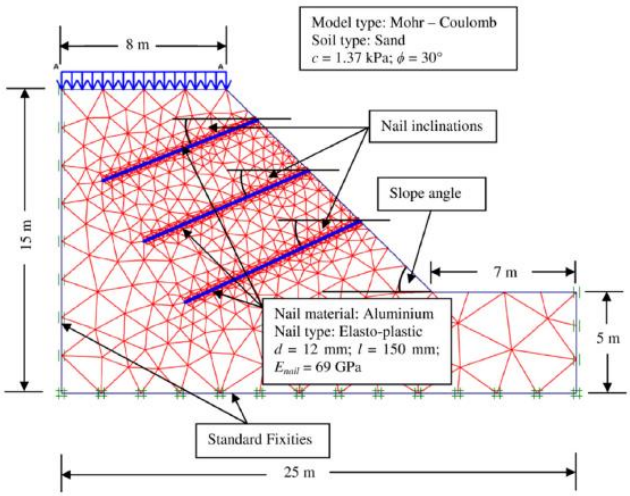

Fig. 6 Numerical modelling of reinforced soil slope in PLAXIS 2D. Rawat S and Gupta AK, (2016)

Table 3 Properties of simulated soil used in numerical modelling (Brinkgreve RBJ, Engin E, Swolfs WM ,2012)

Parameters	Values	Units	Interface strength	
Nail element and nail type	Plate and elastic	–	R_{inter}	2/3
Axial stiffness (EA)	2.98×10^6	kN/m	δ_{inter}	0.1
Flexural rigidity (EI)	113.64×10^3	kN m^2/m		
Diameter of nail (d_{eq})	12	mm		
Poisson's ratio (υ)	0.35	–		

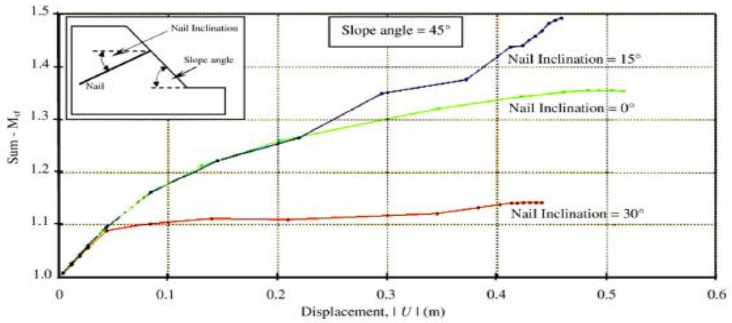

Fig. 7 Factor of safety against slope displacement from PLAXIS 2D for different nail inclinations at 45° slope. Rawat S and Gupta AK, (2016)

3.2 Slip Surface from PLAXIS 2D.

It is observed from the analysis of reinforced slopes using the FEM routine PLAXIS that non-circular slip surface failure occurs on different slopes with changing nail inclination. Though it is discovered that variations in nail inclination cause these slip surfaces to fluctuate. In the

example of a nail inclined at 0 ° for a 45 ° slope, Figure 9a shows that the FEM analysis provides a slip surface passing close to the slope faceFailure of a 45-degree slope with 15- and 30-degree nail inclinations results in a similar pattern of non-circular slip surfaces. Additionally, Fig. 9b, c shows that, in contrast to 0 ° nail inclination, slide surfaces travel through the 15 ° and 30 ° nail inclinations. The highest horizontal displacement, however, is seen to be in close proximity to the strengthened slope face in all three nail inclinations. Compared to 45 ° slopes, the failure pattern of 60 ° slopes exhibits a distinct variation. For a 0 ° nail inclination in a 60 ° slope, as seen in Fig. 10a.

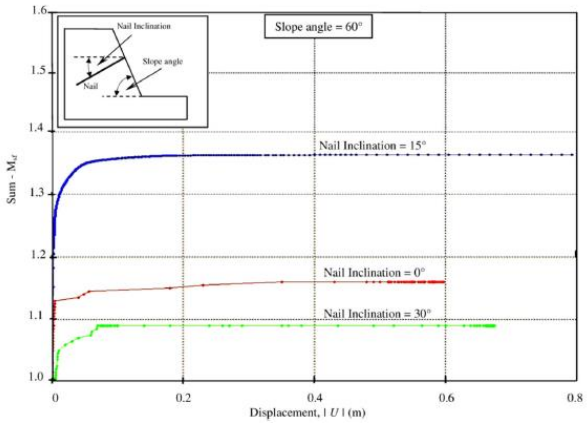

Fig. 8 Factor of safety against slope displacement from PLAXIS 2D for different nail inclinations at 60º slopes. Rawat S and Gupta AK, (2016)

Compared to 45 ° slopes, the failure pattern of 60 ° slopes exhibits a distinct variation. A non-circular slip surface occurs for a nail inclination of 0 degrees on a 60-degree slope, as shown in Fig. 10a. This failure of the slip surface is more akin to the sliding failure. Nevertheless, it is discovered that the surcharge loading has caused the entire crest to shift. The research yields a well-defined slip surface for nail inclinations of 15 º. The slope crest is where the slip surface begins and ends at the toe. It is characterized as a non-linear, non-circular kind of slip surface failure. Additionally, it is evident that the slide surface crossed the nails during failure (Figure 8). Fig. 10c shows a complex failure pattern for a 60 ° slope with 30 ° nail inclinations. In contrast to toe failures found for 0 ° and 15 ° nail inclinations, the slope failure pattern is seen. The higher slope face is where the slip surface, which is a wedge failure, generally occurs. Additionally, a greater amount of the failed wedge is shown to not even be able to pass through the bottom nail. For a slope angle of 60 degrees, it is also discovered that the slope has significantly distorted in comparison to other nail inclinations, undergoing a non-circular slip surface.

Table 4 Factor of safety of LEM and FEM

Slope angles with horizontal (°)	Nail inclinations with horizontal			
	FOS	0°	15°	30°
45	LEM	1.69	1.82	1.20
	FEM	1.36	1.43	1.15
60	LEM	1.50	1.53	1.10
	FEM	1.17	1.37	1.08

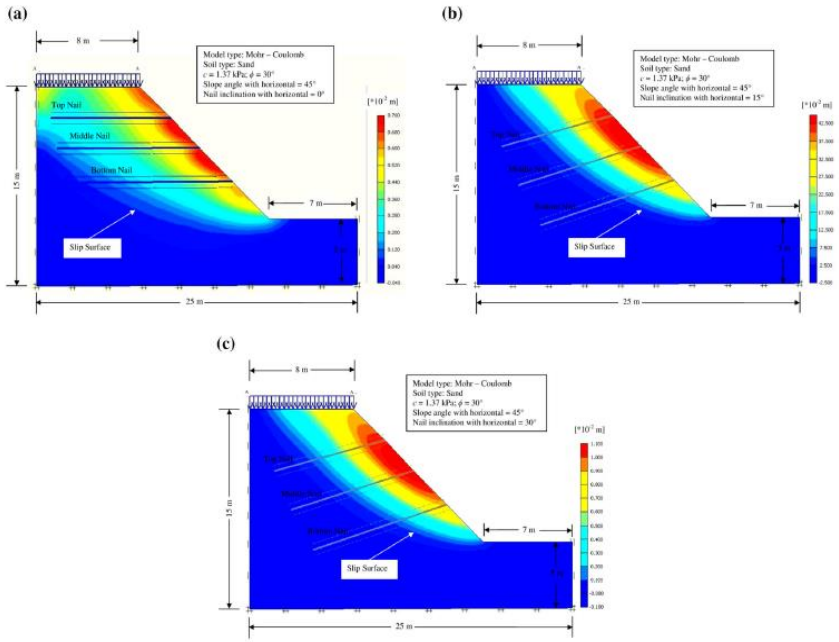

Fig. 9 a Slip Surface at failure for 45 º slope angle from PLAXIS with nail inclination of 0 º. b Slip Surface at failure for 45 º slope angle from PLAXIS with nail inclination of 15 º. c Slip Surface at failure for 45 º slope angle from PLAXIS with nail inclination of 30 º. Ref: Rawat S and Gupta AK, (2016)

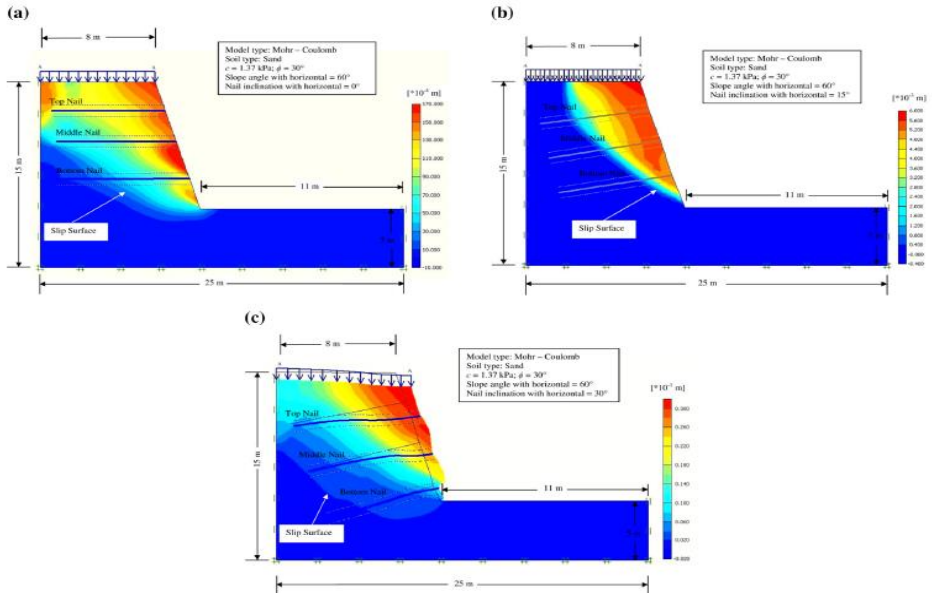

Fig. 10 a Slip Surface at failure for 60 º slope angle from PLAXIS with nail inclination of 0 º. b Slip Surface at failure for 60 º slope angle from PLAXIS with nail inclination of 15 º. c Slip Surface at failure for 60 º slope angle from PLAXIS with nail inclination of 30 º. Ref: Rawat S and Gupta AK, (2016)

4 Discussions

Table 5. Comparison of Finite Element method and Limit Equilibrium Method

Finite Element Method	**Limit Equilibrium Method**
1. Suitable for high complex geometry with degree of high realism	1. Can compute the factor of safety for simple slope geometry with limit equilibrium method
2. Can compute displacement and stresses that caused by the loading for 2D and 3D modes	2. Can only compute in 2D mode while ignoring the 3D modes. Assume the soil layers and parameters to be constant for the overall slopes.
3. Can use to estimates the displacement and construction pore water pressure to adjacent structure	3. The soil mass is assumed to move as a rigid block, with the movement only taking place along the failure surface itself. Does not consider the changes in the pore water pressure with the adjacent structure.
4. It is often difficult to anticipate failure modes, particularly if reinforcement or structural members such as geotextiles, concrete retaining walls, or sheet piles are included.	4. The geotextile, concrete retaining walls or sheet piles are not included. But the failure modes can be counted without the reinforcement.
5. Can show how the stress strain and displacement of the soil when the soil nailing or structure member such as retaining wall are included in the Factor of Safety calculations.	5. Can calculate the Factor of Safety for circular and non- circular method

5 Conclusions

Based on the review of both methods, the conclusions that can be made are as follows: -

1. 1. Compared to the Finite Element Method (FEM), the Limit Equilibrium Method (LEM) forecasts a higher Factor of Safety. For slopes analyzed using both LEM and FEM, the most stable slope is found to be at a 15° soil nail inclination with a horizontal.
2. In the soil nailing load transmission mechanism, both LEM and FEM are able to forecast the limiting circumstances, such as the pulling-out capacity, tensile capacity, or facing capacity.
3. The FEM analysis shows how the interface strength varies with Factor of Safety, but the LEM routine does not provide the interface strength. This could also be the cause of the differences between LEM and FEM analysis results.

Overall conclusions, both FEM and LEM methods have advantages and disadvantages. These two methods give the precise results if both methods are combined. The analysis using the LEM to compute the factor of safety are further enhanced with the Finite Element using PLAXIS 3D in order to compute the stress strain displacement of the soil with added soil nailing or structure member such as retaining wall.

The author would like to acknowledge DTLK grant with grant number (20238001DTLK) for funding this research. This research supports the 17 Sustainable Development Goals under category Goal No 13 Climate Action and Goal No 11 Sustainable Cities and Communities.

References

1. Zhou XP, Cheng H (2013) Analysis of stability of three-dimensional slopes using the rigorous limit equilibrium method. Eng Geol 160:21–33
2. Alejano LR, Ferrero AM, Oyanguren PR, Fernandez MIA (2011) Comparison of limit-equilibrium, numerical and physical models of wall slope stability. Int J Rock Mech Min Sci 48(1):16–26
3. Cheng YM, Zhu LJ (2004) Unified formulation for two-dimensional slope stability analysis and limitations in factor of safety determination. Soils Found 44(6):121–127
4. Zhu DY, Lee CF, Jiang HD (2003) Generalised framework of limit equilibrium methods for slope stability analysis. Geotechnique 53(4):377–395
5. SLOPE/W (2001) A software package for slope stability analysis, Ver. 5. GEO-SLOPE International, Calgary
6. Kim J, Salgado R, Lee J (2002) Stability analysis of complex soil slopes using limit analysis. J Geotech Geoenviron Eng 128(7):546–557
7. Loukidis D, Bandini P, Salgado R (2003) Stability of seismically loaded slopes using limit analysis. Geotechnique 53(5):463–480
8. Farzaneh O, Askari F (2003) Three-dimensional analysis of nonhomogeneous slopes. J Geotech Geoenviron Eng 129(2):137–145
9. Chen Z, Wang X, Haberfield C, Yin JH, Wang Y (2001) A three-dimensional slope stability analysis method using the upper bound theorem: part I: theory and methods. Int J Rock Mech Min Sci 38(3):369–378
10. Chen Z, Wang J, Wang Y, Yin JH, Haberfield C (2001) A three-dimensional slope stability analysis method using the upper bound theorem: part II: numerical approaches, applications and extensions. Int J Rock Mech Min Sci 38(3):379–397
11. Lyamin AV, Sloan SW (2002) Upper bound limit analysis using linear finite elements and non-linear programming. Int J Numer Anal Methods Geomech 26(2):181–216
12. Griffiths DV, Lane PA (1999) Slope stability analysis by finite elements. Geotechnique 49(3):387–403
13. Brinkgreve RBJ, Engin E, Swolfs WM (2012) Plaxis 3D 2012 manual. PLAXIS bv Delft University
14. Yang G, Zhong Z, Zhang Y, Fu X (2015) Optimal design of anchor cables for slope reinforcement based on stress and displacement fields. J Rock Mech Geotech Eng 7(4):411–420
15. Jeon SS (2012) Pull-out tests and slope stability analyses of nailing systems comprising single and multi-rebars with grouted cement. J Central South Univ 19(1):262–272
16. Zhou WH, Yin JH, Hong CY (2011) Finite element modelling of pullout testing on a soil nail in a pullout box under different overburden and grouting pressures. Can Geotech J48(4):557–567
17. Rabie M (2014) Comparison study between traditional and finite element methods for slopes under heavy rainfall. HBRC J10(2):160–168
18. Rawat S, Gupta AK (2016) An Experimental and Analytical Study of Slope Stability by Soil Nailing. Electron J Geotech Eng 21(17):5577–5597

19. Jayanandan M and Chandkaran S (2015). Numerical simulation of soil nailed structures International Journal of Engineering Research & Technology (IJERT), ISSN: 2278-0181,Vol.4 Issue 8
20. Cheuk CY, Ho KKS, Lam AYT (2013) Influence of soil nail orientations on stabilizing mechanisms of loose fill slopes. Can Geotech J 50(12):1236–1249
21. Cheuk CY, Ng CWW, Sun HW (2005) Numerical experiments of soil nails in loose fill slopes subjected to rainfall infiltration effects. Comput Geotech 32(4):290–303
22. Murthy BRS, Babu GLS, Srinivas A (2002) Analysis of prototype soil nailed retaining wall. Gr Improvement 6(3):129–136
23. Babu GLS, Murthy BRS, Srinivas A (2002) Analysis of construction factors influencing the behaviour of soil-nailed earth retaining walls. Proc Inst Civ Eng-Gr Improvement 6(3):137– 143
24. Wei W (2008) Three-dimensional slope stability analysis and failure mechanism. Doctoral dissertation, The Hong Kong Polytechnic University, Hong Kong
25. Zheng YR, Zhao SY, Song YK (2005) Advance of study on the strength reduction finite element method [J]. J Logist Eng Univ 3:1–6
26. Shukha R, Baker R (2008) Design implications of the vertical pseudo-static coefficient in slope analysis. Comput Geotech 35:86–96
27. Gurocak Z, Alemdag S, Zaman MM (2008) Rock slope stability and excavatable assessment of rocks at the Kapikaya dam site, Turkey. Eng Geol 96:17–27
28. Hao J, Wang B (2014) Parameter sensitivity analysis on deformation of composite soil nailed wall using artificial neural networks and orthogonal experiment. Math Probl Eng.doi:10.1155/2013/502362 29. Pei HF, Li C, Zhu HH, Wang YJ (2013) Slope stability analysis based on measured strains along soil nails using FBG sensing technology. Math Probl Eng. doi:10.1155/2013/561360
29. Esmaeili F, Varshosaz M, Ebadi H (2013) Displacement measurement of the soil nail walls by using close range photogrammetry and introduction of CPDA method. Measurement 46(9):3449–3459
30. Lin P, Bathurst RJ, Javankhoshdel S, Liu J (2016) Statistical analysis of the effective stress method and modifications for prediction of ultimate bond strength of soil nails. Acta Geotechnica. doi:10.1007/s11440-016-0477-1
31. Li N, Cheng YM (2014) Laboratory and 3-D-distinct element analysis of failure mechanism of slope under external surcharge. Nat Hazards Earth Syst Sci Discuss 2:5937–5970
32. Griffiths DV, Smith IM, Molenkamp F (1982). Computer implementation of a double-hardening model for sand. In Proc. IUTAM conf. on deformation and failure of granular materials. Delft, pp 213–22
33. Morgenstern NR, Price VE (1965) The analysis of the stability of general slip surfaces. Geotechnique 15(1):79–93
34. Lin H, Xiong W, Cao P (2013) Stability of soil nailed slope using strength reduction method. Eur J Environ Civ Eng 17(9):872–885
35. FHWA (2003). Geotechnical engineering circular No 7—soil nail walls. Report FHWA0- IF-03–017. US Department of Transportation, Federal Highway Administration, Washington, DC.
36. Shiu YK, Chang GWK (2006) Effects of inclination, length pattern and bending stiffness of soil nails on behaviour of nailed structures. GEO Report No.197. Geotechnical Engineering Office, Hong Kong.
37. Fan CC, Luo JH (2008) Numerical study on the optimum layout of soil nailed slopes. Computer Geotech 35(4):585–599
38. Babu GS, Singh VP (2009) Simulation of soil nail structures using PLAXIS 2D. Plaxis Bulletin, (Spring Issue No. 25), pp 16–21